Joint 21st IHPC and 15th IHPS, Melbourne, Australia, February 5-8, 2023

Experimental Investigation on the influence of ambient temperature in a Loop Heat Pipe Battery Thermal Management System

Marco Bernagozzi[1*], Anastasios Georgoulas[1], Nicolas Miché[1], Marco Marengo[1]

[1] *Advanced Engineering Centre, University of Brighton, Brighton, UK*

**Corresponding author email address: m.bernagozzi3@brighton.ac.uk*

Abstract

The authors previously proposed and successfully studied the feasibility of an innovative Battery Thermal Management System (BTMS) relying on Loop Heat Pipes (LHPs) and graphite sheets. LHPs act as thermal vector connecting the bottom of the battery pack and a remote chiller, whilst the graphite sheets allow to achieve satisfactory temperature homogenization of the cells surface, containing the added system weight. This design was developed aiming to improve on fast charge timings, all-electric range and reduce costs and complexity. Preliminary studies revealed the potential of this innovative passive BTMS of providing better performance of an active BTMS using a liquid cold plate. Taking a further step in the direction of practical applications, the present work investigates how the proposed BTMS performs in different ambient temperatures by showing the results of several fast charge and heating tests inside an environmental thermal chamber, with temperatures ranging between -20°C to 50°C. The results showed that the LHP worked in all the tested conditions, and that the detrimental undesired cooling provided by the LHP during heating phase (i.e., 1.2°C) was surpassed by the temperature reduction during the cooling phases (i.e., 3.2°C).

Keywords: Battery Thermal Management; Electric Vehicle; Loop Heat Pipe; Thermal Chamber.

1. Introduction

To solve the great challenge of limiting Earth's global warming, the reduction of Green House Gases (GHG) emissions is of vital importance. This needs to be tackled from various angles, from energy production, sustainable agricultural practices, to improved remanufacturing and recycling of goods. One of the biggest strategies sought to tackle global warming, already in place nowadays, is vehicle electrification.

Electric Vehicles (EVs) bring along several challenges, one of them being the thermal management of the batteries. Temperature is in fact a critical aspect for the performance and operative life of the battery pack. It has been reported that the optimum temperature range for a Li-ion battery (being these the present standard on commercial EVs) is between 25°C and 40°C, with heavy power and capacity losses reported both at higher and lower temperatures. Therefore current EVs need a properly designed Battery Thermal Management System (BTMS), and to achieve this, different cooling technologies are employed [1]. The maximum temperature targets are 40°C for optimum performance, 50°C for acceptable performances [2] and 60°C is set as a safety threshold to prevent the occurrence of disruptive phenomena [3] (e.g., thermal runaway).

In a previous work, the Authors developed [4] a novel BTMS based on Loop Heat Pipes (LHPs) and graphite sheets, aimed at increasing all-electric range of the vehicle whilst reducing cost and charging time. Moreover, the Authors employed for the first time an innovative heat transfer fluid, 3M® Novec® 649, which features extremely low ODP and GWP values, on top of not being toxic nor flammable, reducing in this way the risk posed to human safety as well as pollution [5].

The aim of this work is to investigate how the proposed BTMS performs in different ambient temperatures, taking a step further in the direction of practical application. The goal of this investigation is to understand if the LHP, being a passive device acting as a thermal diode, hence capable of only cooling, can be used also in situation where heating is necessary, without being a burden to performances. To do so, two different layouts, one with LHP and one without, are repeatedly tested inside an environmental chamber, allowing the ambient temperature to range between -20°C to 50°C. This work investigates the BTMS performance during different fast charge and heating conditions, as well as during a bespoke driving cycle including motorway driving and fast charge.

2. Battery Thermal Management System and Design and Experimental Setup

The proposed BTMS design, illustrated in Figure 1, foresees to place an array of LHPs at the bottom of the cells modules forming the battery pack, acting

as thermal vector transferring the excess heat from the cells to a remote chiller (part of the built-in HVAC circuit of the vehicle). Finally, graphite sheets are sandwiched in between the cells to promote cell iso-thermalization and prevent heat spreading from one cell to another.

This BTMS, thanks to the use of LHPs, provides very effective heat removal and allows to reduce the parasitic power consumption, compared to an active BTMS. The Authors already proved that this passive LHP-based BTMS can reduce the cells temperature by more than 3°C, compared to a standard active liquid cold plate BTMS, during aggressive drive cycles and fast charge rates [4].

In the experimental set up, for which a schematic diagram is provided in Figure 2, the battery module is composed of dummy cells, made from 5083-O aluminium plates having the same dimensions as the considered cell type (presented in Table 1 together with the graphite sheets dimensions).

Table 1. Dimension and physical properties of aluminum plates and graphite sheets (RS PRO) used for cell dummy model.

Parameter	Aluminum	Graphite	Units
Thickness	10	0.8	mm
Height	96	96	mm
Width	280	240	mm
$\lambda_{\parallel}$	109	350	W/m·K
$\lambda_{\perp}$	109	10	W/m·K
ρ	2670	1300-1500	kg/m^3
c_p	900	810	J/kg·K

The use of dummy cells is a proven practice already used in literature that allows to minimize the risk of generating excessive thermal stress to a real battery cell, while still evaluating the efficiency of the cooling methods. The LHP was made in copper and its evaporator obtained by Yury Maydanik's company Thercon. The chosen working fluid for the LHP was ethanol, due to its low vapour pressure, as pressures greater than 1 bar would have posed mechanical issues to the LHP evaporator, since it is made by thin copper sheets. Further details of the equipment used in the set up shown below are given in previous publications by the Authors [4].

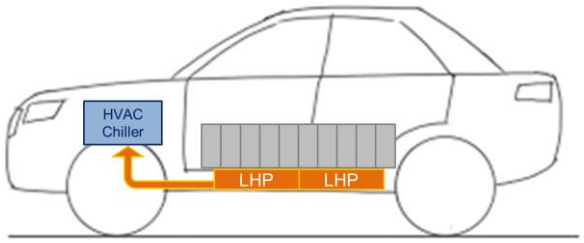

Figure 1. Illustration on the proposed BTMS design idea based on LHPs [4].

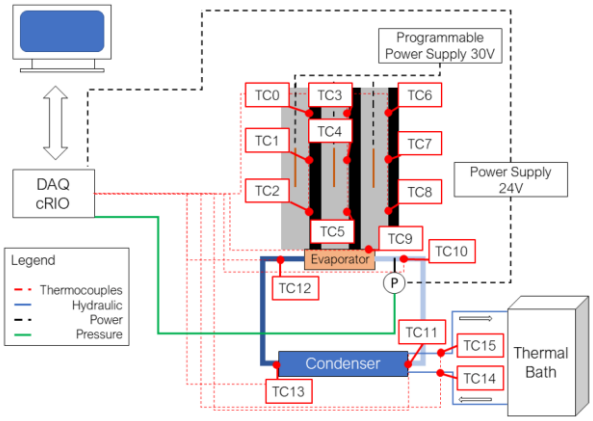

Figure 2. Experimental set up schematic [5].

The experiments are performed in an environmental chamber (TAS, 4.5x4x3.5m, Figure 3) capable of maintain temperatures from -40°C to 60°C with 4kW of internal load. The tests are performed in a temperature range from -20°C to 50°C, to respect the limits imposed by the operative temperature range set by some of the data acquisition instrumentation.

Figure 3. TAS Environmental Chamber used for the tests presented in this work.

3. Experimental Tests

This work is divided in two experimental campaigns, the first one at temperatures lower than

20°C and the second one at higher temperatures. In the first part, the effect of the presence of the LHP during heating from lower temperatures is investigated, with particular interest on establishing and quantifying if the LHP has a detrimental effect on the heating speed and power required to bring the battery module up to 20°C. To do so, tests are repeated heating up the battery module with and without the presence of the LHP at its bottom. The second part investigates the cooling effect of the LHP-based BTMS at high ambient temperatures, to investigate how much its performances are affected by environmental conditions. In Table 2 the proposed test sequence is presented.

Table 2. Experimental test sequence.

#	$T_{amb}[°C]$	LHP
1	-20	w/ LHP
2		no LHP
3	-10	w/ LHP
4		no LHP
5	0	w/ LHP
6		no LHP
7	10	w/ LHP
8		no LHP
10	20	w/ LHP
11		no LHP
12	30	w/ LHP
13		no LHP
14	40	w/ LHP
15		no LHP
16	50	w/ LHP
17		no LHP

The setting up procedure for every test was the same: the thermal chamber was set at the selected ambient temperature and the system was monitored until both the 3-cell module and the LHP reached equilibrium conditions with the ambient. Only then, the heaters were switched on and the data recording started. In other words, in every test the starting temperature of the system was equal to the set ambient temperature.

4. Heating Tests Results

Figure 4 shows the set up equipped with a heater posed on top of the cell. The heater was composed by an aluminium block with two cartridges inserts (Rotfil heating cartridge 36 V, 120 W, 6.5x100 mm). The decision of placing the heating element at the top of the 3-cell module was taken to not move the LHP from the bottom of the module, as main part of the investigation was not to evaluate the efficiency of this heating configuration, but to evaluate if the LHP would have an effect and ultimately quantify it. Moreover, this leaves the door open to evaluate this design by performing numerical simulations in which the bottom surface of the cell module is covered by more LHPs [6], which will be the next step of this investigation.

It was chosen to supply 100 W heating power to the cells, for a duration of 15 minutes, as this would make the module average temperature reach optimum temperature from 0°C (i.e., >25°C).

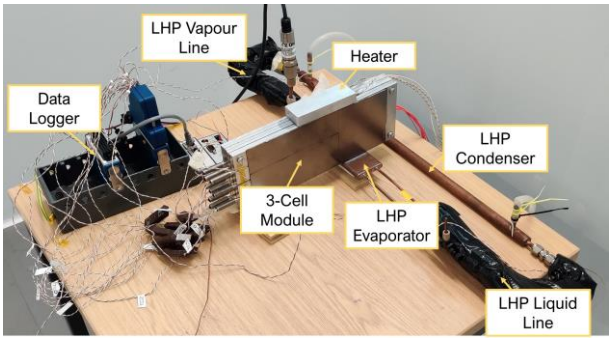

Figure 4. Set up prepared for the heating tests. Aluminum heater with embedded cartridges placed on top of the 3-cell module.

The results in Table 3 show that the presence of the LHP brings about a reduction of the temperature during the heating phase, ranging from 1 to 1.6°C, averaging 1.2°C. This is because the LHP underwent successful start-up even at low temperatures.

Table 3. Results summary of heating tests at low ambient and starting temperature. All temperatures are expressed in °C. $\bar{T}$ stands for average temperature.

LHP	T_{amb}	T_{cell1}	T_{cell2}	T_{cell3}	$\bar{T}$
yes	-20	5.5	-2.2	-1.1	0.7
no		6.1	-0.8	0.1	1.8
Δ		0.6	1.4	1.2	1.1
yes	-10	15.0	7.4	9.0	10.5
no		15.9	9.0	9.9	11.6
Δ		0.8	1.6	1.0	1.1
yes	0	25.0	17.4	19.0	20.5
no		25.6	18.9	19.9	21.5
Δ		0.6	1.5	0.9	1.0
yes	10	35.5	27.4	28.1	30.3
no		36.1	29.5	30.3	32.0
Δ		0.6	2.1	2.2	1.6

5. Cooling Tests Results

5.1. Driving Cycle Tests

The driving cycle considered in these experiments comprised of three sections: a 1C[1] discharge phase (representing fast highway driving), fast charge from 0.2 to 0.8 SOC[2] in 10 minutes, and a final section at 1C discharge. This will be herein referred as HFCH (Highway – Fast Charge – Highway) driving cycle. During the fast charge phase, the maximum charge rate was 4C, which is higher than the state of the art value 3C set by the Porsche Taycan [7]. The considered driving cycle was chosen to foresee future developments in the fast charge section, which will allow the technology to provide a sub-10 minutes charge, being this the target set by industry [8].

The heat power released by the cells are mimicked by flexible heaters inserted in between the aluminium plates, which in turn are controlled by a programmable power supply that can replicate the trends of the heat released by the cells (as shown in Figure 2).

Figure 5 shows the results of the highest temperature test and it is evident from the trends of the evaporator and vapour lines temperatures (TC9, TC10 and TC11, respectively), that start-up took place, even with an ambient temperature of 50°C.

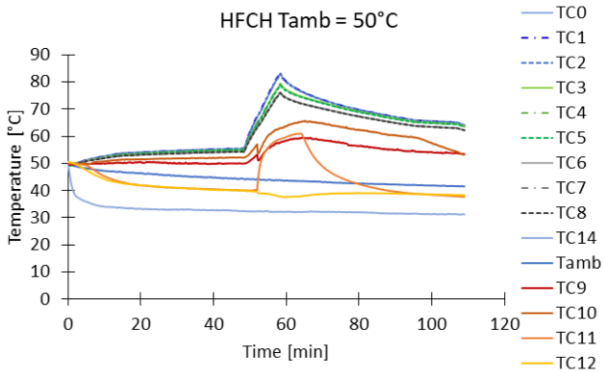

Figure 5. HFCH test results with ambient temperature of 50°C.

In fact, the sudden increase in temperature that the thermocouples see is due to the hot vapour passing through, to signify that the boiling process and fluid circulation have taken place. Regarding the start-up process and how this is influenced by the ambient and starting temperature, the graph in Figure 6 shows that there is a trend between the time needed for the start up to take place and the ambient temperature, when subjected to the same power. The Authors are aware that this is simply a preliminary qualitative case and to draw meaningful conclusions, a more comprehensive testing campaign is needed, perhaps with heat source directly applied to the LHP evaporator (hence without the cells), but this was not the topic of this work.

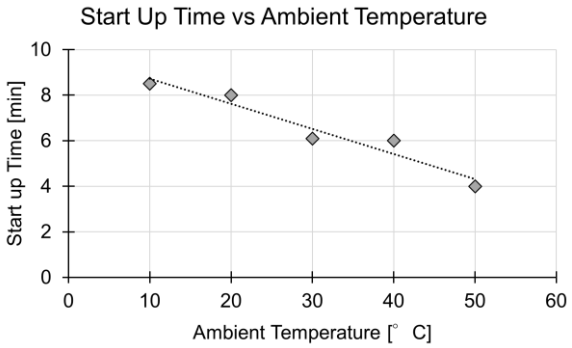

Figure 6. LHP Start-up time at different ambient temperatures.

Nonetheless, it is interesting to note that these results seem to suggest that the system will be more reactive at higher temperatures, which is to be expected from looking at the graphs of *dP/dT* presented in Figure 7. Having high values of *dP/dT* at saturation conditions means that a small change in temperature generates a large change in fluid pressure, augmenting the pumping capability of the bubbles and the whole boiling process [9,10]. Hence, the graphs in Figure 7 explains the results in Figure 6.

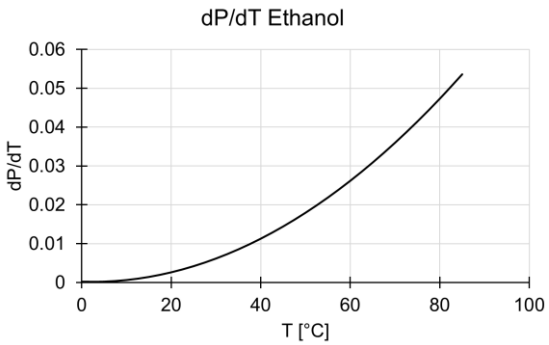

Figure 7. Trend of the derivative of the pressure over temperature ($\boldsymbol{dP/dT}$) at saturation conditions for ethanol.

[1] 1C-Rate is a measure of how quickly a battery is charged or discharged, it is defined as the operating current divided the capacity, e.g. 1C means full charge in 1 hour, 2C in half an hour and so on.

[2] SOC is the State Of Charge, which is a function of the rated capacity and the utilization patterns, denoting the capacity currently available, e.g. SOC 1 means battery full and SOC 0 means battery dead.

Table 4 shows the results of the HFCH tests at different ambient temperatures. Last column also shows that the difference between the maximum temperature and the ambient temperature decreases with the increase of the ambient temperature.

Table 4. HFCH driving cycle tests at different ambient temperatures. All temperatures are expressed in ℃ . $\bar{T}$ is the average module temperature and ΔT is the difference between the $\bar{T}$ and T_{amb}.

T_{amb}	T_{cell1}	T_{cell2}	T_{cell2}	$\bar{T}$	ΔT
10	51.2	47.6	44.6	47.8	37.8
20	59.4	55.5	52.7	55.9	35.9
30	67.4	63.5	60.7	63.9	33.9
40	75.8	71.8	69.1	72.3	32.3
50	83.2	79.2	76.3	79.6	29.6

In all cases it is evident from Table 4 that one LHP is not enough to maintain the cells temperature below the optimum values of 40°C. However, it is enough to keep them below the acceptable and safety thresholds of 50°C and 60°C in the two first cases, respectively.

5.2. Fast Charge at 3C Tests

To appreciate the effect of the single LHP on the battery module temperature evolution during a 3C test, 8 tests were performed at 4 different temperatures (20 °C, 30 °C, 40 °C, 50 °C) with and without the LHP presence. A 3C fast charge will bring the battery SOC from 20% to 80% in 12 minutes. Results are shown in Table 5 and visually in Figure 8.

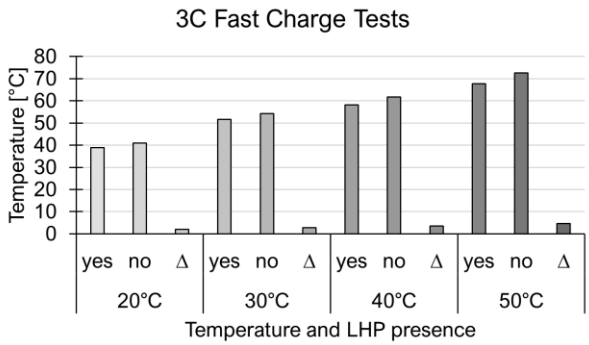

Figure 8. Results of the 3C Fast Charge Tests, in which the battery module' average temperature is compared between cases with or without the LHP, and the relative difference is highlighted.

Table 5. Results from the 3C fast charge tests at high temperatures. The table shows the cells maximum temperatures after fast charge. All temperatures are expressed in °C. $\bar{T}$ stands for average temperature.

LHP	T_{amb}	T_{cell1}	T_{cell2}	T_{cell3}	$\bar{T}$
yes	20	40.7	39.2	37.1	39.0
no		42.9	41.2	39.0	41.0
Δ		2.2	2.1	1.9	2.0
yes	30	53.6	51.7	49.3	51.5
no		56.6	54.2	52.1	54.3
Δ		3.0	2.5	2.8	2.7
yes	40	60.0	58.3	56.2	58.2
no		63.7	61.8	59.5	61.7
Δ		3.7	3.6	3.2	3.5
yes	50	69.7	67.9	65.8	67.8
no		74.7	72.6	70.2	72.5
Δ		4.9	4.8	4.4	4.7

Especially looking at the temperature reduction that the LHP brings compared to the free convection, this Δ value increases with the increase of the ambient temperature.

The true effect of the LHP presence will be evaluated via numerical simulations, in which the coverage of the module footprint will be increased. In fact, in the configuration utilised in this work, only the 17% of the bottom of the module is in contact with the active zone of the LHP evaporator, hence representing a big limitation to the maximum transmissible heat (as a function of the surface).

6. Discussion

Despite the non-optimal temperatures reached by the cells during the different experiments at high ambient temperatures, the LHP demonstrated to be able to work in all conditions, vouching for its applications flexibility. It was already known from previous works by the Authors that this specific evaporator design is not the best suited for the considered battery module geometry. However, it was proven that increasing the size of the evaporator [4] or the number of the evaporators [6] allowed for exceptional thermal performances (i.e., temperature in optimum range even at high fast charge cycles). This works therefore extends the premise of the LHP application to BTMS, suggesting that this technology can produce good results in a wide

range of temperatures, effectively encouraging its adoption in the automotive world.

Figure 9 compares the temperature difference between cases with and without the LHP, during both heating and cooling tests. Since the extra unwanted cooling provided by the LHP is not beneficial during the heating phase, for clarity purposes it is reported with a negative sign on the graph. In this way, the y axis in Figure 9 represents the beneficial effect of the single LHP applied to the 3-cell battery module, compared to free convection only. It shows that during heating phases the ΔT is not dependant from the ambient temperature, and that the LHP presence delays the heating process by 1°C. On other hand, during the cooling phase, the LHP does affect the module's temperature incrementally with the ambient temperature, reaching almost 5°C of difference during the tests at 50°C. It is also intuitive looking at the red and blue areas in the graph in Figure 9 that the advantage provided by the LHP-based BTMS during cooling largely outweighs the decrease in performance during heating. Of course, the true extent of this disparity is to be evaluated with further investigations.

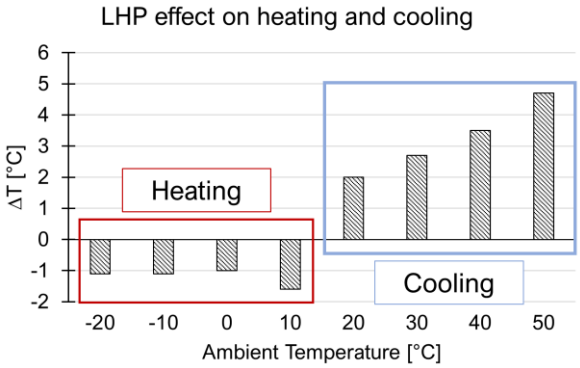

Figure 9. Effect of the LHP presence on the heating and cooling processes. The ΔT value for the heating is represented with a negative sign to signify it is not a positive outcome.

7. Conclusions

In this work, the operation of a LHP-based BTMS was investigated at different ambient temperatures, from -20°C to 50°C, by means of an environmental chamber. Main purpose of this study was to evaluate the effect of the LHP presence during heating and cooling scenarios. Particularly, to understand how much the heating phase would be delayed by the presence of the LHP, and if so, how would this handicap compare to the advantages provided by the device during cooling operations at high temperatures. Several tests were repeated with and without the LHP at the bottom of a 3-cell dummy battery module.

During the heating tests, 100 W were supplied to the module for 15 minutes. For the cooling tests, firstly the conditions of a thermally demanding driving cycle with highway driving and fast charge (HFCH) were replicated, and secondly a 3C fast charge cycle was tested. Each condition was tested at different ambient temperatures: -20°C to 10°C for heating, 20°C to 50°C for cooling. The chosen fluid for the LHP was ethanol.

The main conclusions that can be drawn from the results were:

1. LHP start-up took place at each ambient temperature case; this result advocates for the operational adaptability of this device.
2. During heating, the battery module presents a temperature 1.2°C lower when heated up with the LHP at its bottom, compared to being heated without the LHP; however, this effect seems to be insensitive to the ambient temperature.
3. During the HFCH driving cycle tests, module temperatures were above the safety threshold of 60°C when ambient temperature exceeded 30°C, due to the low heat transfer areas between the two bodies.
4. A qualitative trend emerged between start-up time and ambient temperature, indicating that start-up takes place quicker at higher temperatures; this suggests that a LHP-based BTMS would be naturally quicker to react at higher temperatures, which is a desirable feature.
5. Despite the small dimensions of the LHP active zone, it still provided considerable reduction to the maximum average temperature of the module, from 2°C to 4.7°C lower temperatures than free convection only.
6. Comparing the effect on heating and cooling, the advantage provided by the LHP-based BTMS during cooling clearly outweighs the decrease in performance during heating.

Finally, the results presented herein aim to be foundation to further work in evaluating the feasibility of this LHP-based BTMS idea, in order to go in the direction of an industrial application. Further developments of this study are the investigation of how a design with more LHPs or a larger active LHP evaporator zone affects the module temperature both at heating and cooling phases. In fact, next step foresees a further

validation of the numerical model already developed by the Authors, obtained by matching the results at different ambient temperatures. Following, alternative geometries increasing the heat transfer area between the LHP and the bottom of the battery module will be used in simulations with the same boundary conditions of the tests presented in this work.

Acknowledgments

The Authors would like to thank the Advanced Engineering Centre at the University of Brighton for the access to the environmental chamber and for the economic support obtained to participate to the conference.

References

[1] X. Zhang, Z. Li, L. Luo, Y. Fan, Z. Du, A review on thermal management of lithium-ion batteries for electric vehicles, Energy. 238 (2022) 121652. doi:10.1016/j.energy.2021.121652.

[2] P. Qin, M. Liao, D. Zhang, Y. Liu, J. Sun, Q. Wang, Experimental and numerical study on a novel hybrid battery thermal management system integrated forced-air convection and phase change material, Energy Convers. Manag. 195 (2019) 1371–1381. doi:10.1016/j.enconman.2019.05.084.

[3] P.R. Tete, M.M. Gupta, S.S. Joshi, Developments in battery thermal management systems for electric vehicles: A technical review, J. Energy Storage. 35 (2021) 102255. doi:10.1016/j.est.2021.102255.

[4] M. Bernagozzi, A. Georgoulas, N. Miché, C. Rouaud, M. Marengo, Novel battery thermal management system for electric vehicles with a loop heat pipe and graphite sheet inserts, Appl. Therm. Eng. 194 (2021). doi:10.1016/j.applthermaleng.2021.117061.

[5] M. Bernagozzi, N. Miché, A. Georgoulas, C. Rouaud, M. Marengo, Performance of an Environmentally Friendly Alternative Fluid in a Loop Heat Pipe-Based Battery Thermal Management System, Energies. 14 (2021) 7738. doi:https://doi.org/10.3390/en14227738.

[6] M. Bernagozzi, A. Georgoulas, N. Miché, C. Rouaud, M. Marengo, Comparison Between Different Battery Thermal Management Systems During Fast Charge Cycles, in: 17th UK Heat Transf. Conf., Manchester, UK, 2021: pp. 4–6.

[7] A. Tomaszewska, Z. Chu, X. Feng, S. O'Kane, X. Liu, J. Chen, C. Ji, E. Endler, R. Li, L. Liu, Y. Li, S. Zheng, S. Vetterlein, M. Gao, J. Du, M. Parkes, M. Ouyang, M. Marinescu, G. Offer, B. Wu, Lithium-ion battery fast charging: A review, ETransportation. 1 (2019) 100011. doi:10.1016/j.etran.2019.100011.

[8] S. Kim, T.R. Tanim, E.J. Dufek, D. Scoffield, T.D. Pennington, K.L. Gering, A.M. Colclasure, W. Mai, A. Meintz, J. Bennett, Projecting Recent Advancements in Battery Technology to Next-Generation Electric Vehicles, Energy Technol. 10 (2022). doi:10.1002/ente.202200303.

[9] S. Khandekar, N. Dollinger, M. Groll, Understanding operational regimes of closed loop pulsating heat pipes : an experimental study, Appl. Therm. Eng. 23 (2003) 707–719. doi:10.1016/S1359-4311(02)00237-5.

[10] Y.F. Maydanik, Loop heat pipes, Appl. Therm. Eng. 25 (2005) 635–657. doi:10.1016/j.applthermaleng.2004.07.010.